land

Article

# Topographical Gradient Characteristics of Land-Use Changes in the Agro-Pastoral Ecotone of Northern China

**Qiaoqiao Gong [1], Piling Sun [1,2,3,*], Qingguo Liu [1,2] and Junxiong Mo [1]**

[1] School of Geography and Tourism, Qufu Normal University, Rizhao 276826, China
[2] Rizhao Key Laboratory of Territory Spatial Planning and Ecological Construction, Rizhao 276962, China
[3] College of Land Science and Technology, China Agriculture University, Beijing 100193, China
* Correspondence: spling86@qfnu.edu.cn; Tel.: +86-187-3632-1108

**Abstract:** The agro-pastoral ecotone of northern China (AENC) is a significant ecological barrier, where the topographical features play basic roles in land-use change. In order to reveal the influence of topographical factors on land-use changes in the AENC, we used land-use transfer matrix, geo-information graphics, terrain niche, distribution index and geographical detector to explore the topographic gradient effect of land-use changes during 2000–2020 in the AENC based on remote-sensing image data from 2000, 2010, and 2020. The findings indicate that: (1) The total areas of land-use changes were 121,744 km$^2$, accounting for 17.41% between 2000–2020. This was characterized by increasing amounts of land-use changes in the AENC. The changes in land-use were dominated by the conversions among farmland, forestland, and grassland, which were distributed widely in the mountainous regions of northern, western, and eastern margins. The expansion of construction land was derived mainly from farmland and grassland occurred in river valleys. (2) The pattern of land-use changes was divided into five types including stable type, prophase change, anaphase change, continuous change, and repeated change. Stable type accounted for 559,868.86 km$^2$ and 80.09% of the total area. It was dominant in high altitude and complex terrain areas with terrain niches of more than 1.61. Prophase and anaphase changes accounted for 3.95% and 13.03%, respectively, which occupied to dominant positions in the 0.69–1.17 and 0.04–0.69, 1.17–1.61 terrain niches topographic gradient, respectively. Continuous and repeated changes occupied dominant positions in low altitude and flat complex areas with terrain niches of 0.04–1.17. (3) The topographic gradient effect of land-use changes in the AENC was influenced comprehensively by natural, geographical location, socioeconomic, and policy factors. Natural environmental factors and geographical location determined the topographic gradient pattern of land-use structure, while the direction of the topographical gradient pattern of land-use changes in the AENC is influenced by socioeconomic and policy factors. This research can provide a scientific reference for the development and protection of territorial space and optimal allocation of land resources in the AENC.

**Keywords:** land-use change; topographic gradient; geo-information graphics; agro-pastoral ecotone of northern China (AENC)

check for updates

**Citation:** Gong, Q.; Sun, P.; Liu, Q.; Mo, J. Topographical Gradient Characteristics of Land-Use Changes in the Agro-Pastoral Ecotone of Northern China. *Land* **2022**, *11*, 2195. https://doi.org/10.3390/land11122195

Academic Editor: Adrianos Retalis

Received: 22 October 2022
Accepted: 2 December 2022
Published: 3 December 2022



## 1. Introduction

With the persistent improvement of social economies, human society has an increasingly profound impact on the natural environment. Land-use/cover change (LUCC) is a direct reflection of the role how human activities affect natural ecosystems and is connected to land surface material circulation, biodiversity, and sustainable utilization of resources and environment [1,2]. Land use could easily change between and within classes, driven by a combination of natural environment, social economy, and policy factors [3–5]. Given that human production and economic activities often occur in low terrain areas, the ecological policies mainly focus on ecological fragile areas with complex terrain [6–8]. Socioeconomic activities and policies have a topographic gradient effect on land-use changes. As a basic natural geographical element, topographic factors have a direct effect on the migration and energy conversion of surface substances and to some extent, determine the direction and method of land use [9–11]. With the intensification of contradiction between human and land, three-dimensional use mode of land resources has emerged as a hot topic in the research of global environmental change and sustainable development. Numerous scholars have focused on the influence of topographic factors on the selection of agricultural regions, and regional LUCC and its ecological effects under the constraints of elevation conditions [5,12–14]. Moreover, topographic factors such as altitude, slope, and terrain relief constitute the foundation for the formation of land-use pattern, which has an important impact on LUCC. The connection between topographic factors and land-use change has emerged as an essential component of LUCC research [15]. The topographic gradient effect of land-use change is emphasized in land-change science, particularly in delicate and ecologically important regions [10,16,17]. Against the background of ecological civil construction, it is crucial to pay attention to the influence of topographic factors in sensitive and fragile areas with extremely important ecological environment on the spatiotemporal heterogeneity of land-use change, and to build a new pattern of territorial space development and protection, regulate human activities reasonably, and carry out land ecosystem management and control according to local conditions.

Numerous studies have analyzed the land-use change, land-use function, or ecological effect in sensitive and fragile areas using Landsat data in the context of ecological civil construction strategy [18–20]. Currently, the spatial pattern and optimal allocation of land use in sensitive and fragile areas are attracting widespread attention in academic circles, with previous studies mainly focusing on the impact of topographic factors on the selection of agricultural location, regional LUCC and its ecological effect under elevation constraints, and the topographic gradient effect of land-use pattern change [2,17,21]. With the implementation of regional coordinated development and an ecological civil construction strategy, urban marginal areas, the Yellow River Basin, the Yangtze River Basin, the Beijing-Tianjin-Hebei region, and the agro-pastoral ecotone of northern China (AENC) have become areas of extreme interest for research on land-use change [19,20,22–24]. Using technologies such as remote sensing, geographic information systems, and computer mapping, geo-information graphics can vividly and dynamically display the process of land-use change in graphic units as a spatiotemporal composite analysis method. Geo-information graphics are used widely in research on land-use pattern change [10,21,24], but there have been a few studies using geo-information graphics on the spatiotemporal heterogeneity of land-use structure and pattern related to topographic factors in the entire AENC [10,25–29].

In China, agricultural production is roughly bounded by the 400 mm annual precipitation isoline (i.e., from the Greater Hinggan Mountains, Tongliao, Zhangbei, Yulin, Lanzhou, Yushu to the vicinity of Lhasa), which can be divided into two regions: the east and the south are agricultural areas dominated by planting, while the west and the north are pastoral areas dominated by animal husbandry. Between these two regions, there is agro-pastoral ecotone that spreads along the northeast southwest, farming and animal husbandry coexist in space and alternate in time. Located at the junction of the western part of the Northeast Plain and the eastern portion of the Inner Mongolia Plateau and extending to the north of the Loess Plateau in the southwest, the AENC is an important ecological barrier to curb desertification eastward and southward, which is a typical ecologically fragile area in China. As of late, with the fast improvement of society and economy in the AENC, natural issues such as vegetation annihilation, land debasement, and soil disintegration are expanding, and clashes between environmental security and monetary advancement are becoming progressively self-evident, where land use has changed significantly over the past two decades as a result of China's rapid industrialization and urbanization as well as ecological projects such as converting farmland to forest or grass. It is therefore urgent to clarify the law of land-use changes for the overall perspective of the AENC, so as to provide support for ecological protection and coordinated development. Previous studies related to land-use changes in the AENC mainly focused on change in and simulation of land-use pattern [27], optimal allocation of land use [30,31], habitat quality and ecological risk assessment [25,32], and driving factors of land-use change [33]. Many studies emphasized particular parts of the AENC, such as the Loess Plateau [26,28,34–36], the North Hebei mountains [37], the poverty belt around Beijing and Tianjin [10,38], and the arid area of northern China [39]. However, the spatiotemporal characteristics and topographic gradient effect of land-use change in the whole AENC have so far been ignored.

The primary objectives of this study are to (i) explore the spatiotemporal characteristics of land-use transitions during 2000–2020 in the AENC, (ii) reveal the impact of terrain on land-use changes, and (iii) explore the causes of the topographic gradient effect of land-use changes. The results of this study will serve as a scientific reference for the AENC's development, protection of territorial space and optimal allocation of land resources.

## 2. Materials and Methods

### *2.1. Study Area*

The AENC connects the western portion of the Northeast Plain with the eastern portion of the Inner Mongolia Plateau, and it stretches northwest to the Loess Plateau in the north. However, there is as yet no unified understanding of the scope and boundary of the AENC. Since Zhao Songqiao first proposed the idea of an agro-pastoral ecotone, different scholars have proposed the AENC from different perspectives. The present study determines the scope and boundary of the AENC according to the studies of Wang et al. (1999) and Ma et al. (2015) [40,41]. The location is 34°43′31″–46°57′46″ N, 100°57′11″–125°34′11″ E, which includes 226 counties (banners, cities, districts) in Inner Mongolia, Jilin, Liaoning, Hebei, Shanxi, Shaanxi, Gansu, Ningxia, and Qinghai provinces (autonomous regions). The total area is 699,078.78 km$^2$ and is inclined from southwest to northeast. The elevation ranges −160–4973m above sea level (Figure 1). Plateau, mountains, and hills are dominant in this area. Low temperatures, drought, and little precipitation characterize the temperate semi-arid and arid climate of the AENC. The annual average temperature is 0–8 °C, the annual average precipitation is 300–450 mm, and the rate of variation of the annual precipitation is high, ranging from 15 to 30% [42]. The vegetation gradually shifts from a forest steppe zone to a desert steppe zone as precipitation decreases from east to west. The ecological environment of the AENC is typically sensitive and fragile, but it is also an important element of the "two barriers and three belts" strategic pattern of ecological security in China, which is a significant ecological barrier to curb desertification eastward and southward. By the end of 2019, there were more than 70 million people living there, which is an important ecological pointer for establishing regional ecological security in China.

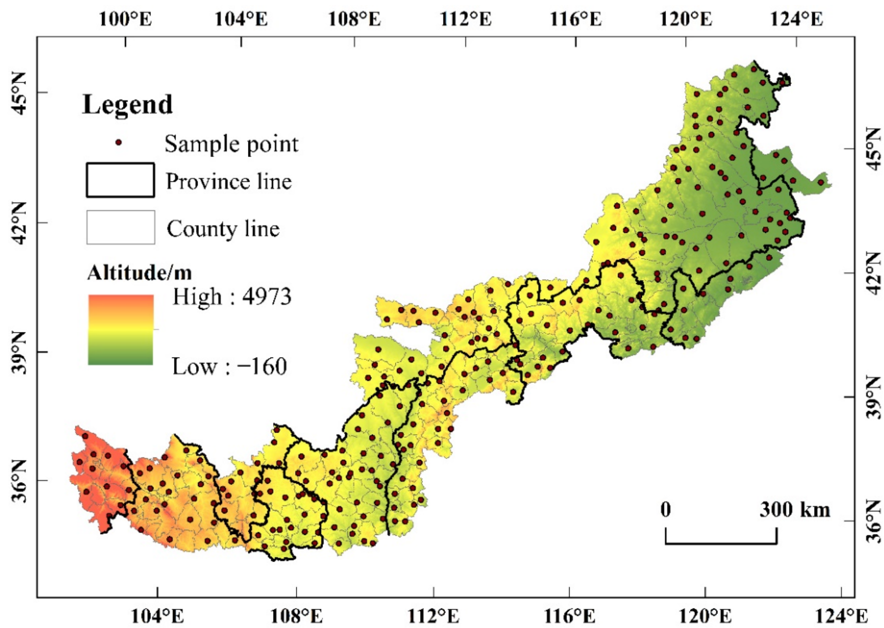


**Figure 1.** Location of study area.

### *2.2. Data Sources and Processing*

The data used in this study include remote sensing images, topographic data, meteorological data, soil data, and socioeconomic data (Table 1).

**Table 1.** Main data types and sources.

| Data Types | Data Sources | Data Resolution |
|---|---|---|
| Landsat TM images (2000, 2010)<br>Landsat OLI images (2020) | Geo-spatial Data Cloud (http://www.gscloud.cn/), (accessed on 1 April 2021). | 30 m × 30 m<br>15 m × 15 m |
| Meteorological data | China Meteorological Science Data Sharing Service Network (http://cdc.cma.gov.cn/), (accessed on 1 April 2021). | 1 km × 1 km |
| Soil data (Soil thickness) | China data set of the World Soil Database (HWSD). | 500 m × 500 m |
| Digital elevation model (DEM) | Resource and Environmental Science and Data Center (http://www.resdc.cn/), (accessed on 1 April 2021). | 30 m × 30 m |
| Socioeconomic statistics | Statistical Yearbooks, Statistical Communiques, and China County Statistical Yearbooks of provinces and cities in the AENC. | - |

The Landsat images were preprocessed with ENVI 5.1 atmospheric correction and geometric rectification. The following steps were taken to interpret the Landsat images: Initially, 281 ground test focuses were gathered and grouped in August 2020 with Google Earth and spot looking over. For the purpose of evaluating the accuracy, approximately 35% of the sample points were chosen at random. Second, the images were interpreted and categorized using neural-net estimation and man-machine interactive interpretation techniques. Thirdly, the results were tested and verified. For the images from 2000, 2010, and 2020, respectively, overall accuracies of 87.68%, 89.72% and 88.59% were obtained. The kappa coefficients for the same years were 0.85, 0.87, and 0.86, indicating that the interpretation results could meet the requirements of this study [10,19]. The land-use types used in this study were farmland, forestland, grassland, water, construction land, and unused land based on the classification system for national resources and the environmental context (Figure 2). Fourth, meteorological data were interpolated onto raster-formatted surfaces with a resolution of 1 km × 1 km using the tension spline method [42]. A digital elevation model (DEM) was used to obtain the topographical data. From the DEM, slope and terrain relief were taken. The DEM, slope and terrain relief were divided into five levels based on the study area's actual surface morphology (Table 2). By using smoothing calculations or substituting data from adjacent years, partial missing data were obtained. Finally, the above data were digitized, geometric correction, mask clipping, format conversion and uniformly projected based on the ArcGIS software platform, and all of the data were unified to the resolution of 1 km × 1 km to establish basic database of the AENC.

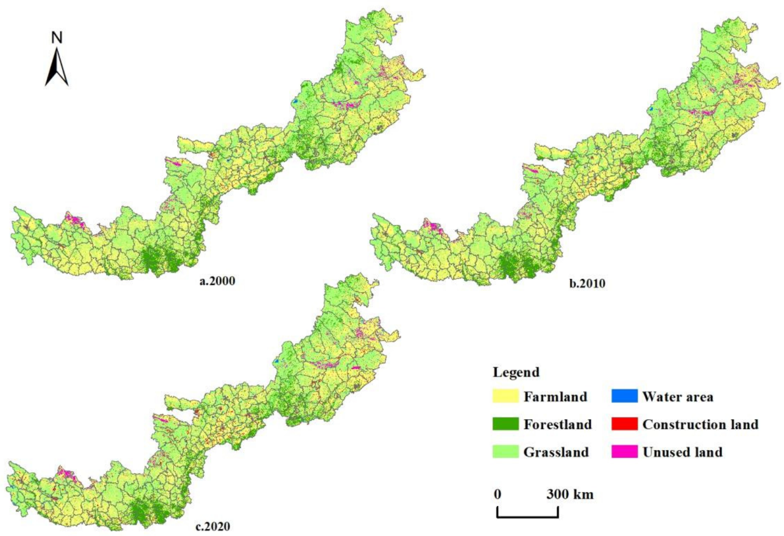


**Figure 2.** Land-use maps within AENC in 2000, 2010, and 2020.

**Table 2.** Classification and area proportion of digital elevation model (DEM), slope, and terrain relief.

| Rank | Elevation | | Slope | | Terrain Relief | |
|---|---|---|---|---|---|---|
| | Classification (m) | Proportion (%) | Classification (°) | Proportion (%) | Classification (m) | Proportion (%) |
| I | <200 | 6.96 | <2 | 16.32 | <50 | 19.86 |
| II | 200–500 | 12.81 | 2-6 | 30.11 | 50–100 | 17.06 |
| III | 500–1000 | 17.24 | 6–15 | 32.19 | 100–200 | 51.57 |
| IV | 1000–3500 | 62.09 | 15–25 | 16.29 | 200–300 | 7.76 |
| V | >3500 | 0.90 | >25 | 5.09 | >300 | 3.75 |

## 2.3. Methods

### 2.3.1. Land-Use Transfer Matrix

The land-use transfer matrix quantitatively displays the quantity and direction of land-use conversion among different land-use types in different periods [43]. The interconversion relationship between land-use types in the AENC was analyzed using the land-use transfer matrix in this research during 2000–2020. It is expressed as [19]:

$$T_{ij} = \begin{bmatrix} T_{11} & T_{12} & \cdots & T_{1\mathrm{n}} \\ T_{21} & T_{22} & \cdots & T_{2n} \\ \cdots & \cdots & \cdots & \cdots \\ T_{n1} & T_{n2} & \cdots & T_{nn} \end{bmatrix} \tag{1}$$

where $T_{ij}$ (km$^2$) is the area converted from land-use type $i$ to land-use type $j$, and $n$ is the number of land-use types.

### 2.3.2. Importance Index of Land-Use Change

The importance index of land-use change was used to screen out the main types of land-use change in the AENC. It is expressed as [44]:

$$N_p = Y_p/Y \times 100\% \tag{2}$$

$$Y = \sum\nolimits_{p=1}^{m} Y_p \tag{3}$$

where $N_p$ (range: [0, 100%]) is the importance index of land-use change type $p$, $Y_p$ (km$^2$) is the area of change type $p$, and $Y$ is the sum area of the AENC's land-use change. The larger the value of $N_p$, the more dominant the land-use change. The main types of land-use changes were then selected according to the rank of $N_p$.

### 2.3.3. Geo-Information Graphics

Geo-information graphics vividly and dynamically display the process of land-use change in graphic units with the technologies of remote sensing, geographic information systems, and computer mapping and were used to represent the information about land-use change during 2000–2020 in the AENC. The calculation formula is [24]:

$$M = A \times 100 + B \times 10 + C \tag{4}$$

where $M$ is the land-use change pattern model, while $A$, $B$, and $C$ are the land-use types in 2000, 2010, and 2020, respectively. Based on the change characteristics of land-use graphic units, five types of change patterns were obtained (Table 3), i.e., prophase change, anaphase change, continuous change, repeated change, and stable type [10]. Prophase change referred to changes in land-use structure occurring in 2000–2010 and remaining unchanged in 2010–2020. Anaphase change meant that land-use structure remained unchanged in 2000–2010 and changed during 2010–2020. Continuous change indicated that land-use changes occurred in 2000–2010 and 2010–2020, and land-use types were different in 2000 and 2020. Repeated change indicated that land-use changes occurred in 2000–2010 and then returned to 2000 use in 2020. Stable type meant that land-use remained unchanged during 2000–2020.

**Table 3.** Geo-information graphics of land-use change during 2000–2020 in the AENC.

| Types | Meaning | Sample |
|---|---|---|
| Stable type | Land-use structure didn't change during 2000–2020. | Grassland-Grassland-Grassland |
| Prophase change | Land-use structure changed only in 2000–2010. | Forestland-Grassland-Grassland |
| Anaphase change | Land-use structure changed only in 2010–2020. | Grassland-Grassland-Farmland |
| Continuous change | Changes occurred during 2000–2010 and 2010–2020. | Grassland-Forestland-Farmland |
| Repeated change | Change occurred in 2000–2010 and then returned to 2000 use in 2020. | Farmland-Grassland-Farmland |

#### 2.3.4. Terrain Niche

The terrain niche index (TNI), created by combining elevation and slope, revealed the spatial distribution characteristics of the land-use pattern on the terrain position gradients [5]. It is expressed as [10,25]:

$$TNI = \ln\left[\left(\frac{E}{E_0}+1\right)\times\left(\frac{S}{S_0}+1\right)\right] \tag{5}$$

where $E$ (m) is the elevation of the pixel, $E_0$ (m) is the average elevation; $S$ (°) is the slope of the pixel, and $S_0$ (°) is the average slope. The higher the elevation and the greater the slope, the greater the value of *TNI*. The terrain niche of the AENC was divided into the five grades of I [0.04, 0.69), II [0.69, 1.17), III [1.17, 1.61), IV [1.61, 2.09), and V [2.09, 3.52]) with Jenks natural breaks.

#### 2.3.5. Distribution Index

To eliminate the effect of topographic gradients, the distribution index (DI) was used to describe the land-use change on topographic gradients. A common dimensionless index, the DI is expressed as [45]:

$$DI = \left(SA_{kq}/SA_k\right)/\left(SA_q/TA\right) \tag{6}$$

where $SA_{kq}$ (km$^2$) is the area of land-use change pattern $k$ on terrain niche $q$, $SA_k$ (km$^2$) is the area of land-use change pattern $k$, $SA_q$ (km$^2$) is the area of terrain niche $q$, and $TA$ (km$^2$) is the total area of the study area. When $DI > 1$, terrain niche $q$ is dominant in land-use change pattern $k$, and the larger the value of $DI$, the greater the dominance.

#### 2.3.6. Geographical Detector

The factor detection module of the geographic detector is utilized to identify the driving factors of land-use structure change in AENC. It is expressed as [46]:

$$q = 1 - \frac{1}{n\sigma^2}\sum_{h=1}^{L} n_h \sigma_h^2 \tag{7}$$

where, $n$ and $\sigma^2$ are the total number of sample units and variance, $n_h$ and $\sigma_h^2$ are the number of units and variance of layer $h$, and $L$ is the total number of layers of the driving factor. $q$ is the influence of each driving factor, whose value range is [0, 1].

Land-use structure change was driven by the natural environment, geographical location, social economy and regional policies [10,23,34]. Land-use change are based on natural environmental factors. Differences in topography, climate and soil factors will lead to uneven distribution of land resources, population and industrial structure. The difference of geographical location determines the pattern of spatial distribution of geographical elements, and the distribution of rivers (water resources) and town center affects the direction of land utilization. Socioeconomic factors are important driving forces of land-use change. Social and economic development and land-use status interacts and influence each other. Regional policies regulate the distribution of natural resources and human activities. Under the background of ecological civilization construction and food security, a series of national policies have a significant impact on land-use change in the AENC. In order to explore the driving factors of land-use structure changes, we selected main areas of land-use changes as dependent variables. Referring to the existing research, we selected explanatory variables from those four dimensions, i.e., natural environment, geographical location, socioeconomic and regional policy factors (Table 4). Natural environment factors in the AENC were characterized by five explanatory variables including elevation, slope, mean annual precipitation, annual mean temperature, soil thickness. Geographical location condition in the AENC was characterized by two explanatory variables including distance to the nearest river and distance to county capital. Socioeconomic factors in the AENC were characterized by six explanatory variables including grain yield, year-end large livestock stock, number of agriculture employee, population density, economic density, and road network density. Two explanatory variables of ecological conversion and basic farmland protection were selected to embody the regional policy.

**Table 4.** Driving factors of land-use structure change in the AENC.

| **Driving Factors** | | **Explanatory Variables** | **Interpretation** |
|---|---|---|---|
| Natural environment factors | Topographic condition | X1 Elevation | Digital elevation model (DEM) of each unit (m). |
| | | X2 Slope | Slope of each unit (°). |
| | Climate condition | X3 Mean annual precipitation | ArcGIS software was used to spatially interpolate the annual mean precipitation for each unit(mm). |
| | | X4 Annual mean temperature | ArcGIS software was used to spatially interpolate the annual mean temperature of each unit (°C). |
| | Soil condition | X5 Soil thickness | Soil reference depth of each unit (cm). |
| Geographical Location | | X6 Distance to the nearest river | Distance of cells to the nearest river (km). |
| | | X7 Distance to county capital | Distance of cells to the county capital (km). |
| Socioeconomic factors | | X8 Grain yield | Total grain yield in the region ($\times 10^4$ t). |
| | | X9 Year-end large livestock stock | Number of large livestock stocks in the region at the end of the calendar year ($\times 10^4$ head). |
| | | X10 Number of agriculture employee | Number of people engaged in agriculture in the region (person). |
| | | X11 Population density | Total population was divided by total regional area ($\times 10^9$ person/km$^2$). |
| | | X12 Economic density | Gross domestic product was divided by the total regional area ($\times 10^9$CNY/km$^2$). |
| | | X13 Road network density | Road mileage was divided by the total regional area (km/km$^2$). |
| Regional policy factors | | X14 Ecological conversion | During 2000–2020, if one unit of conversion from farmland to forestland, grassland or water area assigned the value of 1, or 0 otherwise. |
| | | X15 Basic farmland protection | If one unit was located in a basic farmland protection area, assigned the value of 1, or 0 otherwise. |

## 3. Results

### *3.1. Land-Use Changes in AENC*

#### 3.1.1. Changes in Land-Use Structure

The majority of land-use types in the AENC were farmland, forestland, and grassland, as shown in Figure 2 and Table 5, whose area proportion decreased from 96.22% in 2000 to 94.48% in 2020. Meanwhile, typical patterns of land use were formed by the spatial variation in the distribution of farmland, forestland, and grassland in the AENC. From 2000 to 2020, the area of grassland decreased from 328,162.6 km$^2$ to 313,629.72 km$^2$, with a rate of change of 4.43%, which was spread primarily in the mountainous regions of the northern, eastern, and western margins as well as the low mountainous and hilly area of the Loess Plateau. Grassland was the largest land-use type in the area during 2000–2020. The area of farmland increased by 0.19%, from 268,959.49 km$^2$ to 269,471.62 km$^2$ over the study period, primarily distributed in the valleys of Huangshui, Yellow River, and Daqing River, located in Qinghai, Gansu, Ningxia, and Inner Mongolia. The area of forestland increased from 75,547.52 km$^2$ to 77,359.96 km$^2$ during 2000–2020, at a rate of change of 2.40%, primarily distributed in the southern margin. The largest positive change was found for construction land, with a rate of change of 118.63%, which occurred mainly in the river valleys and intermountain basins.

**Table 5.** Dynamic changes in land-use types during 2000–2020 in the AENC.

| Land-Use Types | 2000 | 2010 | 2020 | 2000–2020 | |
|---|---|---|---|---|---|
| | Area (km$^2$) | Area (km$^2$) | Area (km$^2$) | Change Area (km$^2$) | Change Rate (%) |
| Farmland | 268,959.49 | 264,216.49 | 269,471.62 | 512.13 | 0.19 |
| Forestland | 75,547.52 | 75,435.97 | 77,359.96 | 1812.44 | 2.40 |
| Grassland | 328,162.60 | 332,665.41 | 313,629.72 | −14,532.90 | −4.43 |
| Water | 4367.72 | 3287.45 | 4614.36 | 246.64 | 5.65 |
| Construction land | 9541.74 | 10,991.71 | 20,861.47 | 11,319.73 | 118.63 |
| Unused land | 12,499.62 | 12,481.72 | 13,141.65 | 642.03 | 5.14 |

3.1.2. Changes in Land-Use Conversion

Changes in AENC land-use types over the past 20 years were further calculated by superimposing 2000–2020 land-use maps (Table 6 and Figure 3). Farmland, forestland, grassland, and unused land were substantially converted during 2000–2020. From 2000 to 2010, there were 30 types of land-use change in the AENC, with a conversion area of 48,060.69 km$^2$, accounting for 6.87% of the total area. The first nine types accounted for 90.23% of the land-use change area and were the main process of land-use types conversion. In total, 11,699.20 km$^2$ of farmland were converted to grassland, accounting for 24.34% of the land-use change area, which was the most significant. It was mainly distributed in the mountainous area of the northern and eastern margins of the junction among Inner Mongolia, Hebei, and Liaoning. The decreased forestland was mainly converted to grassland, accounting for 9142.60 km$^2$ with an importance index of 19.02%, which ranked second and mainly distributed in the northern mountains of Hebei Province. Overall, 17.92%, 15.38%, 2.76%, and 2.16% of grassland were converted to forestland, farmland, unused land, and construction land, respectively. The third most frequently converted land-use was the conversion of grassland to forestland, which was concentrated in the Qinghai–Tibet Plateau, Loess Plateau, and Bashang Plateau intersection areas. The conversion of grassland to farmland ranked fourth and was mainly concentrated in the Liaohe River Plain, river valleys, and intermountain basins with relatively flat topography. The new construction land mainly came from farmland and grassland, which accounted for 1730.73 km$^2$ and 1035.93 km$^2$, respectively.

**Table 6.** Importance index of land-use changes in the AENC during 2000–2020.

| ID | 2000–2010 | | | 2000–2020 | | |
|---|---|---|---|---|---|---|
| | Conversion Types | Area (km$^2$) | $N_i$ (%) | Conversion Types | Area (km$^2$) | $N_i$ (%) |
| 1 | Farmland-Grassland | 11,699.20 | 24.34 | Grassland-Farmland | 33,470.63 | 30.01 |
| 2 | Forestland-Grassland | 9142.64 | 19.02 | Farmland-Grassland | 20,878.26 | 18.72 |
| 3 | Grassland-Forestland | 8613.02 | 17.92 | Grassland-Forestland | 14,679.14 | 13.16 |
| 4 | Grassland-Farmland | 7389.44 | 15.38 | Forestland-Grassland | 12,973.33 | 11.63 |
| 5 | Farmland-Construction land | 1730.73 | 3.60 | Farmland-Construction land | 8115.65 | 7.28 |
| 6 | Unused land-Grassland | 1386.84 | 2.89 | Grassland-Unused land | 3664.55 | 3.29 |
| 7 | Grassland-Unused land | 1327.49 | 2.76 | Grassland-Construction land | 3321.32 | 2.98 |
| 8 | Construction land-Farmland | 1036.64 | 2.16 | Farmland-Forestland | 2991.23 | 2.68 |
| 9 | Grassland-Construction land | 1035.93 | 2.16 | Unused land-Grassland | 2780.18 | 2.49 |
| 10 | Other 21 types | 4698.76 | 9.78 | Other 21 types | 8657.84 | 7.76 |
| — | Total | | 100 | Total | | 100 |

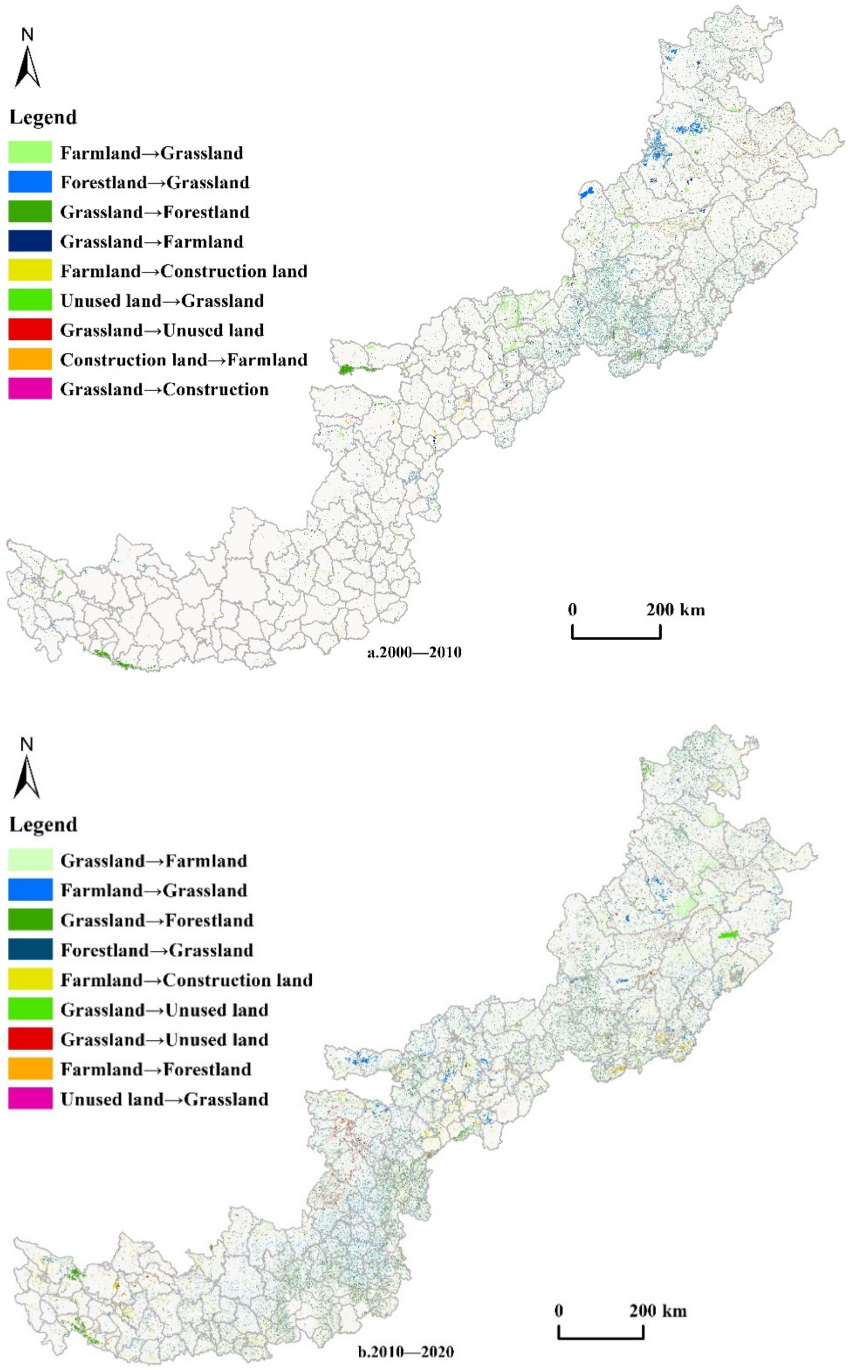


**Figure 3.** Main conversion types of land-use change in the AENC during 2000–2020.

From 2010 to 2020, 30 types of land-use change occurred in the AENC, and the convert area was 111 532.13 km2, accounting for 15.95% of the total area, and the spatial distribution changed greatly (Figure 3b). As shown in Table 6, the main conversion types of land-use change were characterized by the mutual conversion among farmland, forestland, grassland, and unused land. The first nine types represented 92.24% of the total area changed. The conversion from grassland to farmland accounted for 33,470.63 km$^2$ and 30.01% of the total area changed during 2010–2020, making it the most significant conversion type. It was mainly spread in the mountainous region of the northern and eastern margins in the junction among Inner Mongolia, Jilin, Hebei, and Liaoning as well as the low mountainous and hilly area of the Loess Plateau. In addition, the decreased grassland was turned to forestland, unused land, and construction land, accounting for 13.16%, 3.29%, and 2.98% of the total land-use change area, respectively. The conversion from farmland to grassland ranked second with an area of 20,878.26 km$^2$, accounting for 18.72% of the total land-use change area, which was primarily distributed in low mountainous and hilly area of the Loess Plateau, Bashang Plateau, and the mountainous area of the northern and eastern margins. The conversion areas of forestland and unused land to grassland were 12,973.33 km$^2$ and 2780.18 km$^2$, respectively, but the decrease in grassland did not balance the area of forestland and unused land converted to grassland. As China's new industrialization and urbanization process accelerates, the expansion of construction land mainly derived from farmland and grassland. Urban districts and the areas surrounding them in river valleys and intermountain basins saw the majority of the conversion of farmland to construction land. Moreover, 2991.23 km$^2$ of farmland were converted to forestland because of the construction of the farmland shelterbelt.

### *3.2. Topographical Gradient Effect of Land-Use Structure Change in the AENC*

According to the spatial analysis, the geo-information of the land-use structure change in the AENC from 2000 to 2020 is shown in Figure 4 and Table 7.

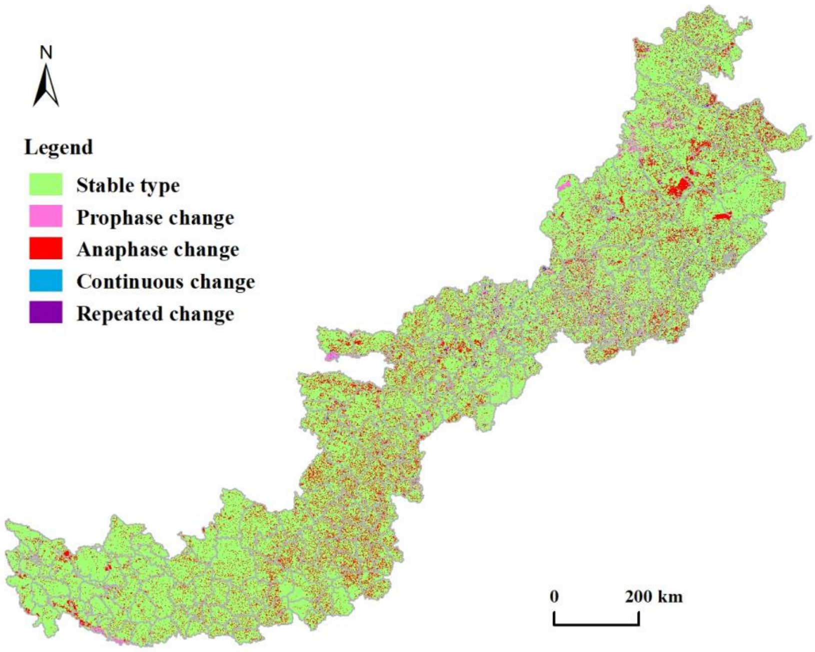


**Figure 4.** Geo-information of land-use structure change in the AENC during 2000–2020.

The spatial pattern of land-use structure change was obviously different in the AENC. The stable type of land-use structure change was the most widespread in the AENC and accounted for 559,868.86 km$^2$ and 80.09% of the total area during 2000–2020. The largest types of stable land-use structure were "grassland–grassland–grassland" and "farmland–farmland–farmland", which accounted for 46.90% and 40.36%, respectively, of the total area of stable types. Grassland and farmland were dominant in the mountainous areas of the northern and eastern margins and valley basins in the AENC during 2000–2020. Moreover, the "grassland–grassland–grassland" type was distributed mainly in high-altitude and complex terrain areas located in Donghai, Lanzhou, Yullin, Chifeng, Tongliao, Ulanhot City, and Chengde City, while "farmland–farmland–farmland" happened mainly in Xining, Lanzhou, Datong, Shuozhou, the southeastern area of Jining, and the southern area of Tongliao City with relatively low and flat terrain. The area of prophase change was 27,635.00 km$^2$, accounting for 3.95% of the total area. The "forestland–grassland–grassland" type occurred mainly in the Inner Mongolia Plateau and its surrounding areas such as Kshketan Banner, Bahrain Left Banner, Arukorqin Banner, Zarut Banner, west of Horqin Right Front Banner, Chengde County, and Pingquan County. Meanwhile, "farmland–

grassland–grassland" occupied dominant positions in the junction among Inner Mongolia, Hebei, and Shanxi including Taiservant Temple Banner, Kangbao, Zhangbei, Guyuan, Duolun, Wuchan, and Shanyin County. The anaphase change types such as "grassland–grassland–farmland" and "farmland–farmland–grassland/ construction land" accounted for 91,080.59 km$^2$ and 13.03% of the total area. The continuous change type of land-use structure covered an area of 3010.81 km$^2$ and 0.43% of the total area. The change type of "grassland–forestland–farmland" was dominant in the continuous change type of land-use structure, which primarily existed in the southern areas of Guyang and Wuchuan County. The repeated change type of land-use structure covered an area of 17,413.61 km$^2$, which accounted for 2.49% of the total area. The main change type of land-use structure was "farmland–grassland–farmland" with 30.35% of the total area of repeated change type in the AENC during 2000–2020.

**Table 7.** Geo-information graphic type of land-use structure change in the AENC during 2000–2020.

| Change Types | Land-Use Structure Changes | | Largest Types of Geo-Information Graphics | |
|---|---|---|---|---|
| | Area (km$^2$) | Proportion (%) | Sample | Proportion of Change Types (%) |
| Stable type | 559,868.86 | 80.09 | Grassland-Grassland-Grassland | 46.90 |
| | | | Farmland-Farmland-Farmland | 40.36 |
| Prophase change | 27,635.00 | 3.95 | Forestland-Grassland-Grassland | 23.03 |
| | | | Farmland-Grassland-Grassland | 21.37 |
| Anaphase change | 91,080.59 | 13.03 | Grassland-Grassland-Farmland | 30.38 |
| | | | Farmland-Farmland-Grassland | 19.34 |
| Continuous change | 3010.81 | 0.43 | Grassland-Forestland-Farmland | 11.88 |
| Repeated change | 17,413.61 | 2.49 | Farmland-Grassland-Farmland | 30.35 |

Correlation analysis was utilized to measure the connections between the topographic factors. The correlation coefficients were 0.968, 0.893, 0.592, 0.688, 0.738, and 0.892, indicating that there were close relationships between elevation and terrain relief, elevation and terrain niche, elevation and slope, slope and terrain relief, slope and terrain niche, and terrain niche and terrain relief, respectively (Table 8).

**Table 8.** The interrelationships between topographic factors.

| Topographic Factors | Elevation | Slope | Terrain Relief | Terrain Niche |
|---|---|---|---|---|
| Elevation | / | | | |
| Slope | 0.592 ** | / | | |
| Terrain relief | 0.986 ** | 0.688 ** | / | |
| Terrain niche | 0.893 ** | 0.738 ** | 0.892 ** | / |

Note: ** represents the significance level of 1%.

Due to the extreme correlation of those topographic factors, the topographical gradient characteristics of land-use structure changes were very similar. Therefore, we selected the terrain niche to investigate the topographical gradient effect of land-use structure changes in the AENC (Figure 5). It showed an uptrend of stable type of land-use structure as topographic factors increased, and its dominant distribution area was mainly distributed at terrain niche index exceeded 1.17. These areas had an elevation of more than 1000 m, and a slope of more than 6°, where the terrain relief exceeded 100 m. Meanwhile, the DI of prophase change and anaphase change type fluctuated obviously. The DI of prophase change type was located mainly in areas with a terrain niche index between 0.69 and 1.17, while anaphase change type occupied the dominant position at terrain niche index of 0.04–0.69 and 1.17–1.61. Moreover, the types of continuous change and repeated change occurred mainly in low altitude and flat terrain areas with a terrain niche index less than 1.17, where there was an elevation of less than 1000 m, a slope within 6°, and a terrain relief of less than 100 m. In these areas, the DI of continuous change and repeated change type were greater than 1.

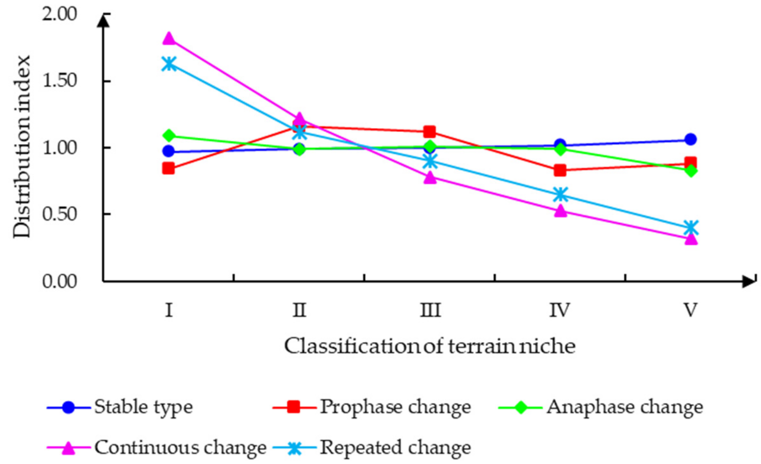


**Figure 5.** DI of terrain niche gradient for land-use structure changes.

### *3.3. Driving Factors of Land-Use Structure Change in the AENC*

The study's driving factors for changes in the AENC's land-use structure were investigated using geographical detector. The findings demonstrated that changes in land-use structure were influenced by the natural environment, geographical location, social economy and regional policy (Table 9).

**Table 9.** Driving factors of land-use structure changes in the AENC.

| Driving Factors | Stable Type | | Prophase Change | | Anaphase Change | | Continuous Change | | Repeated Change | |
|---|---|---|---|---|---|---|---|---|---|---|
| | Grassland-Grassland-Grassland | Farmland-Farmland-Farmland | Forestland-Grassland-Grassland | Farmland-Grassland-Grassland | Grassland-Grassland-Farmland | Farmland-Farmland-Grassland | Grassland-Forestland-Farmland | Grassland-Farmland-Construction Land | Farmland-Grassland-Farmland | Farmland-Unused Land-Farmland |
| Elevation | 0.243 *** | 0.439 *** | 0.327 *** | 0.146 *** | 0.361 *** | 0.154 *** | 0.287 *** | 0.311 *** | 0.474 *** | 0.152 *** |
| Slope | 0.214 *** | 0.300 *** | 0.133 *** | 0.176 *** | 0.355 *** | 0.284 *** | 0.165 *** | 0.115 *** | 0.302 *** | 0.230 *** |
| Mean annual precipitation | 0.211 *** | 0.154 *** | 0.125 *** | 0.073 *** | 0.323 *** | 0.320 *** | 0.126 *** | 0.148 *** | 0.229 *** | 0.067 *** |
| Annual mean temperature | 0.450 *** | 0.149 *** | 0.299 *** | 0.490 *** | 0.158 *** | 0.154 *** | 0.228 *** | 0.265 *** | 0.290 *** | 0.107 *** |
| Soil thickness | 0.108 *** | 0.157 *** | 0.114 *** | 0.055 *** | 0.203 *** | 0.154 *** | 0.101 *** | 0.138 *** | 0.228 *** | 0.067 *** |
| Distance to the nearest river | 0.252 *** | 0.089 *** | 0.131 *** | 0.080 *** | 0.173 *** | 0.095 *** | 0.152 *** | 0.133 *** | 0.163 *** | 0.132 *** |
| Distance to county capital | 0.734 *** | 0.216 *** | 0.446 *** | 0.265 *** | 0.560 *** | 0.282 *** | 0.341 *** | 0.254 *** | 0.402 *** | 0.089 *** |
| Grain yield | 0.305 *** | 0.725 *** | 0.273 *** | 0.145 *** | 0.557 *** | 0.261 *** | 0.332 *** | 0.395 *** | 0.601 *** | 0.166 *** |
| Year-end large livestock stock | 0.348 *** | 0.490 *** | 0.367 *** | 0.187 *** | 0.521 *** | 0.257 *** | 0.390 *** | 0.260 *** | 0.468 *** | 0.181 *** |
| Number of agriculture employee | 0.247 *** | 0.541 *** | 0.252 *** | 0.084 *** | 0.252 *** | 0.192 *** | 0.211 *** | 0.173 *** | 0.289 *** | 0.130 *** |
| Population density | 0.699 *** | 0.125 *** | 0.402 *** | 0.227 *** | 0.462 *** | 0.229 *** | 0.253 *** | 0.165 *** | 0.254 *** | 0.069 *** |
| Economic density | 0.346 *** | 0.147 *** | 0.171 *** | 0.112 *** | 0.174 *** | 0.144 *** | 0.088 *** | 0.067 *** | 0.141 *** | 0.055 *** |
| Road network density | 0.238 *** | 0.238 *** | 0.131 *** | 0.116 *** | 0.271 *** | 0.254 *** | 0.136 *** | 0.069 *** | 0.208 *** | 0.152 *** |
| Ecological conversion | 0.117 *** | 0.129 *** | 0.117 *** | 0.120 *** | 0.168 *** | 0.283 *** | 0.070 *** | 0.220 *** | 0.123 *** | 0.090 *** |
| Basic farmland protection | 0.076 *** | 0.127 *** | 0.016 ** | 0.043 *** | 0.009 * | 0.005 | 0.003 | 0.032 *** | 0.001 | 0.025 *** |

Note: ***, ** and * indicate significant correlations at the 0.01, 0.05 and 0.10 levels, respectively.

#### 3.3.1. Natural Environment Factors

As shown in Table 9, land-use structure changes in the AENC were resulted from topographic conditions, climate conditions and soil conditions. The distribution of grassland

and land-use structure changes from farmland to grassland and forestland mainly occurred in the areas with high elevation. The mutual conversion between farmland and grassland was significantly influenced by elevation, and the explanatory power was greater than 0.3, which was significant at the 1% level. In addition, the explanatory power of elevation on the transformation of farmland to construction land was 0.311. The effect of slope on farmland, grassland-grassland-farmland and farmland-grassland-farmland was greater, which were 0.300, 0.355 and 0.302, respectively. The mean annual precipitation had great influence on the grassland-grassland-farmland and farmland-farmland-grassland. The pattern of farmland-grassland-grassland and grassland distribution was significantly influenced by the annual mean temperature. Moreover, soil thickness had a strong influence on the conversion from farmland to grassland.

#### 3.3.2. Geographical Location Factors

As shown in Table 9, the distribution of grassland was significantly influenced by the distance to the nearest river and the distance to county capital, and the explanatory power was 0.252 and 0.734, respectively, which was significant at the 1% level. In addition, it had a strong influence on the transition from grassland to farmland, such as grassland-grassland-farmland and farmland-grassland-farmland, among which the explanatory power of distance to county capital was greater than 0.4. Among other things, the effect of distance to county capital on the conversion from forestland to grassland was 0.446, which is significant at the 1% level.

#### 3.3.3. Socioeconomic Factors

As shown in Table 9, grain yield and year-end large livestock stock had a great influence on the distribution of farmland and grassland-grassland-farmland with explanatory power of more than 0.4. The distribution of farmland was significantly influenced by the number of agricultural employees, and the explanatory power was 0.541, which was significant at the 1% level. With an explanatory power of 0.699 and 0.346, respectively, the distribution of grassland was strongly influenced by population density and economic density. In addition, population density also had a strong influence on forestland-grassland-grassland and grassland-grassland-farmland. Road network density mainly affects grassland, farmland, grassland-grassland-farmland, farmland-farmland-grassland and farmland-grassland-farmland.

#### 3.3.4. Regional Policy Factors

The effect of ecological conversion policy on farmland-farmland-grassland and grassland-farmland-construction land was significant, with explanatory power of 0.283 and 0.220, respectively, which was significant at the 1% level. In addition, the explanatory power of ecological conversion policy on grassland-grassland-farmland was also strong, which was 0.168. The policies of farmland protection had significant influences on the spatiotemporal evolution of farmland. Since 2000, with the advancement of food security strategy, more attention had been paid to the protection of the quantity, quality and ecology of farmland. As shown in Table 9, the spatial distribution of stable farmland was strongly influenced by basic farmland protection, and the explanatory power was 1.27, which was significant at the 1% level.

## 4. Discussion

### *4.1. Topographical Gradient Effect and Driving Factors of Land-Use Structure Change in the AENC*

Topographical gradient effect of land-use structure changes was influenced by the combination of geographical environment, socioeconomic and regional policy factors. Geographical environment, including the natural environment and geographical location, affected the topographic gradient pattern of land-use structure, while the changes in land-use pattern were resulted from social economy and regional policy.

#### 4.1.1. Geographical Environment Determines the Topographic Gradient Pattern of Land-Use Structure

The topographic gradient pattern of land-use changes is typically either boosted or resisted by natural environment factors, which are the foundation of land-use pattern evolution in the AENC. The results indicated that natural environment basically determined the spatial distribution pattern of land-use cover and changes in the AENC. The impact of topographic conditions on land-use distribution and change has been concerned by many scholars. Similar results were reported from Sun et al. and Li et al., who found that the topographic gradient effect of land-use structure changes resulted from terrain relief and terrain niche [10,29]. In the 21st century, ecological policies and ecological projects have been carried out in the AENC, resulting in the land-use changes in farmland-grassland-grassland and farmland-forestland-grassland in high altitude and complex terrain areas with elevations exceeding 1000 m and slopes of more than 15°. Moreover, many existing studies revealed that topographic factors played important roles in the redistribution of surface water and thermal conditions, as well as soil conditions [10,27,32,47].

The advantages and disadvantages of location conditions have a certain impact on land-use changes in the AENC; it determines the spatial distribution pattern of geographical elements, which lay the foundation for land-use allocation. AENC was located in arid and semi-arid region where water resources have an important impact on farmland reclamation and livestock development. With the progress of science and technology, agricultural irrigation technology had been improved and promoted, and the restrictive effect of water resources on farmland reclamation became smaller. Liu and Li's investigation of China's northern border transect yielded the same conclusion [48].

#### 4.1.2. Socioeconomic Conditions Are Key Driving Forces of Land-Use Changes

In the AENC, the spatiotemporal evolution of land-use structure is significantly influenced by socioeconomic factors. The spatiotemporal evolution of the land-use pattern was influenced by population agglomeration, economic development, urbanization process, and the construction of transportation. Population growth was one of main driving factors in promoting the increase in farmland [49]. Additionally, areas with more agricultural employees have a more stable spatial distribution of farmland. In the main grain producing areas, grassland and unused land are more easily converted to farmland, while in pastoral areas, the distribution of grassland is more stable, and forestland is more easily converted into grassland. Economic development was an important factor in stimulating the transformation of farmland to construction land. During the last 20 years, rapid development of economic and urbanization level, structure of industry upgrade, and urban population growth has led to land-use changes which have occurred mainly in low altitude and flat terrain region, and mainly located in Xining, Lanzhou, Datong and Shuozhou City (Figures 2 and 3). By the end of 2020, the total population had exceeded 70 million, of whom 83.11% were distributed in low-altitude and flat terrain areas with elevations between 0–1500 m, slopes between 0–25°, and terrain reliefs between 0–200 m. During the same time, the urbanization rate increased by nearly 15% in the AENC. With the acceleration of urbanization and much of rural population migrating to urban areas, farmland has been indirectly abandoned [35,45]. The total areas of farmland converted to forestland, grassland, and water areas were 3240.69 km$^2$, 23,751.22 km$^2$, and 625.99 km$^2$ during 2000–2020, respectively. Considering the topographical conditions, economic activities were concentrated in low-altitude and flat terrain areas, where construction land constantly occupied farmland in a terrain niche of less than 1.17 (Figure 5). It was characterized by change types of farmlands and grassland-farmland-construction land. Meanwhile, farmland spread to areas with higher topographic gradients to meet food demand in the AENC. The change types of grassland-grassland-farmland and unused land-unused land-farmland happened mainly in complex terrain areas with a terrain niche of 1.17–1.61 (Figure 3). The present results were basically consistent with those from previously studies in the AENC [26,34,45,50].

4.1.3. Regional Policy Regulates Land-Use Allocation

Policy factors reflect the government's basic guidance on economic development and land resource allocation, which are important driving forces for the spatiotemporal evolution of topographic gradient pattern of land-use changes [34,45,51–53]. Macro-control of regional policy factors is mainly reflected in two aspects. On the one hand, it affects the distribution of socioeconomic activities and thus affects the allocation of land-use. On the other hand, it guides the land-use pattern and modifies the land pattern initially determined by natural factors. The topographic gradient effect of changes in land-use in the AENC was significantly affected by ecological policies [34]. This was mainly due to the complexity of natural environment and socioeconomic development and the particularity of human-land relationship in the AENC, as well as the function of national ecological barriers to curb desertification and conserve water [10,42]. Additionally, ecological projects such as the Three-North Shelter Forest Phase IV Project, the Beijing–Tianjin Sandstorm Source Control Project, and the Taihang Mountain Greening Project have had significant effects on the development of the AENC's topographic gradient pattern of land-use as part of the ecological civilization strategy. Forestland and grassland have been restored in the areas with high terrain gradient and complex terrain, which expanded toward lower terrain gradients during 2000–2020. The mountainous regions of the northern, western, and eastern margins, in addition to the low mountainous and hilly regions of the Loess Plateau, saw the majority of the conversion of farmland to grassland and forestland [26,39,54,55]. Given the 2022 Winter Olympics held in Beijing and Zhangjiakou, the topographic gradient pattern of land use has a drastic change (Figure 3).

To sum up, the interaction of natural environmental factors, geographical location, socioeconomic factors, and policy factors resulted in the topographical gradient effect of land-use changes in the AENC, which was a complex and dynamic evolution process. Natural environmental factors and geographical location determined the topographic gradient pattern of land-use structure, while socioeconomic and policy factors affected the direction of topographical gradient pattern of land-use changes in the AENC (Figure 6).

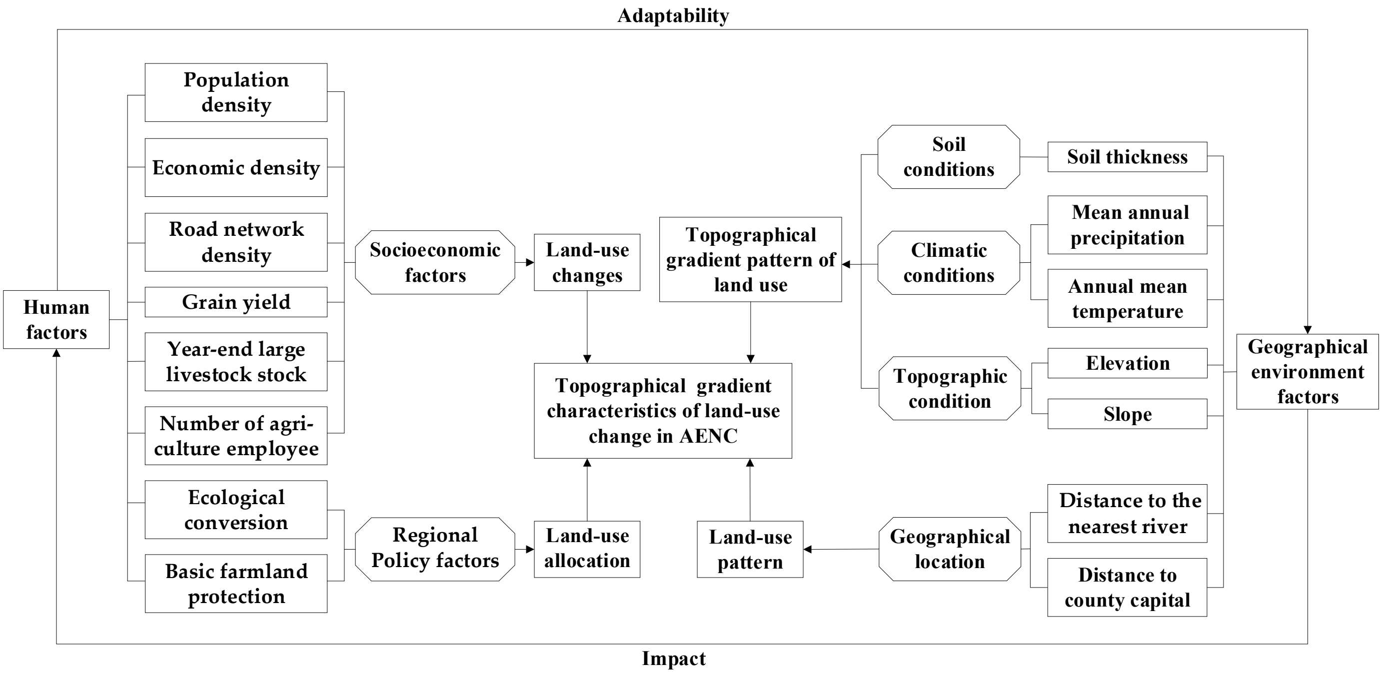


**Figure 6.** Driving mechanism of topographical gradient effect of land-use change in the AENC.

### *4.2. Limitations and Implications*

Limited by the lag of statistical data publication in China, most social and economic data in the AENC was only updated to 2020, while only a few counties located in the AENC were updated to 2021, and most relevant data were not available in 2022. Therefore, the study was only updated to 2020. As a result, the study was only studied until 2020. The "Grain for Green" policy had a significant impact on the AENC's spatiotemporal variations of the topographical gradient pattern of land-use changes. Ecological projects such as the Three-North Shelter Forest Phase IV and V Project, the Beijing-Tianjin Sand-storm Source Control Project, and the Taihang Mountain Greening Project have had significant effects on the evolution of the topographic gradient pattern of land use since 1999, when the ecological civilization strategy was implemented in the AENC. Combined with the evolution of the policy of "Grain for Green", we divided the research period into two stages—2000–2010 and 2010–2020—to explore the spatial heterogeneity of land-use structure changes in the AENC. Therefore, we attempted to investigate the topographic gradient effect of AENC land-use changes between 2000 and 2020. A geographical detector was utilized to investigate the influence of the geographical environment, socioeconomic, and regional policy factors on the topographical gradient pattern of changes in land-use structure in the AENC. A geographical detector was able to probe both numerical and qualitative data without relying on linear assumptions [46]. Using the geographical detector, good results were obtained at a scale of 1 km $\times$ 1 km in this study. Additionally, there are still some uncertainties in this study. To reflect the socioeconomic conditions, only grain yield, year-end large livestock stock, number of agriculture employee, population density, economic density, road network density was chosen given the availability of data in the AENC. Considering that socioeconomic data took the administrative unit as the basic statistical unit and meteorological data came from the observation of meteorological stations, it was difficult to unify data accuracy and research scale. After many tests, it was found that by selecting 1 km $\times$ 1 km grid, the research unit was analyzed best. Furthermore, owing to most policy and system factors were difficult to quantify, the policy of ecological conversion and basic farmland protection were selected to explore the macro-control of regional policy factors on land-use allocation in the AENC. What's more, this study did not pay much attention to the transition characteristics of the AENC, which mainly focused on the vertical direction of land-use changes in the AENC.

In this study, the methods of geo-information graphics, distribution index and geographical detector were used to realize the effective integration of land-use pattern and evolution process and reveal the trend and direction of land-use structure changes in different topographic gradients. The hierarchical distribution law of land-use changes and the topographic gradient effect can be utilized to direct the modification of land-use structure in accordance with local conditions. The low topographic gradient is where the majority of farmland and construction land is distributed. It is also an important area for comprehensive development, where the connection between economic growth and ecological environment protection should be considered. The key goal is to reasonably guide the urbanization process and prevent the loss of farmland. Forestland, grassland, and unused land are dominant in high topographic gradient areas, where agricultural production should be restricted, natural vegetation should be protected, and ecological protection policies should be strictly implemented.

## 5. Conclusions

In the context of ecological civilization construction and rapid urbanization, topographic gradient effect of land-use changes is intensifying, and new patterns of territorial space development and protection are facing challenges. In light of this, based on remote-sensing image data from 2000, 2010, and 2020, this study explored the spatiotemporal pattern and topographic gradient effect of land-use changes in the AENC. The findings are as follows.

(1) The total areas of land-use changes were 121,744 km$^2$, accounting for 17.41% between 2000-2020. It was characterized by increasing amounts of land-use changes in the AENC. The changes in land-use were dominated by the conversions among farmland, forestland, and grassland, which were distributed widely in the mountainous regions of

northern, western, and eastern margins. The expansion of construction land was derived mainly from farmland and grassland occurred in river valleys.

(2) The pattern of land-use changes was divided into five types including stable type, prophase change, anaphase change, continuous change, and repeated change. Stable type accounted for 559,868.86 km$^2$ and 80.09% of the total area. It was dominant in high altitude and complex terrain areas with terrain niches of more than 1.61. Prophase and anaphase changes accounted for 3.95% and 13.03%, respectively, which occupied to dominant positions in the 0.69–1.17 and 0.04–0.69, 1.17–1.61 terrain niches topographic gradient, respectively. Continuous and repeated changes occupied dominant positions in low altitude and flat complex areas with terrain niches of 0.04–1.17.

(3) The topographic gradient effect of land-use changes in the AENC was comprehensively influenced by natural, geographical location, socioeconomic, and policy factors. Natural environmental factors and geographical location determined the topographic gradient pattern of land-use structure, while the direction of the topographical gradient pattern of land-use changes in the AENC is influenced by socioeconomic and policy factors.

**Author Contributions:** Conceptualization, Q.G. and P.S.; methodology, Q.G.; software, J.M.; validation, P.S. and Q.L.; formal analysis, P.S. and Q.L.; investigation, Q.G., P.S., Q.L. and J.M.; writing—original draft preparation, Q.L. and J.M.; writing—review and editing, Q.G. and P.S.; supervision, P.S. All authors have read and agreed to the published version of the manuscript.

**Funding:** This research was funded by National Natural Science Foundation of China (No. 42101258), Ministry of Education Humanities and Social Youth Foundation of China (No. 19YJCZH144), Natural Science Foundation of Shandong (No. ZR2019QD006) and the National College Student Innovation Training Project (202210446004).

**Institutional Review Board Statement:** Not applicable.

**Informed Consent Statement:** Not applicable.

**Data Availability Statement:** The datasets used in this article can be obtained by readers after the article is published online.

**Conflicts of Interest:** The authors declare no conflict of interest.

## References

1. Mooney, H.; Duraiappah, A.; Larigauderie, A. Evolution of natural and social science interactions in global change research programs. *Proc. Natl. Acad. Sci. USA* **2013**, *110*, 3665–3672. [CrossRef] [PubMed]
2. Zang, H.; Liu, Y.; Yang, Y. Land use pattern change and its topographic gradient effect in the mountainous areas: A case study of Jinggangshan city. *J. Nat. Resour.* **2019**, *34*, 1391–1404.
3. Lambin, E.; Turner, B.; Geist, H.; Agbola, S.; Angelsen, A.; Bruce, J.; Coomes, O.; Dirzo, R.; Fischer, G.; Folke, C.; et al. The causes of land-use and land-cover change: Moving beyond the myths. *Glob. Environ. Chang.* **2001**, *11*, 261–269. [CrossRef]
4. Turner, B.; Lambin, E.; Reenberg, A. The emergence of land change science for global environmental change and sustainability. *Proc. Nat. Acad. Sci. USA* **2007**, *104*, 20666–20671. [CrossRef]
5. Xue, L.; Zhu, B.; Wu, Y.; Wei, G.; Liao, S.; Yang, C.; Wang, J.; Zhang, H.; Ren, L.; Han, Q. Dynamic projection of ecological risk in the Manas River basin based on terrain gradients. *Sci. Total Environ.* **2019**, *653*, 283–293. [CrossRef]
6. Matasov, V.; Prishchepov, A.V.; Jepsen, M.R.; Müller, D. Spatial determinants and underlying drivers of land-use transitions in European Russia from 1770 to 2010. *J. Land Use Sci.* **2019**, *14*, 362–377. [CrossRef]
7. Zaehringer, J.G.; Atumane, A.; Berger, S.; Eckert, S. Large-scale agricultural investments trigger direct and indirect land use change: New evidence from the Nacala corridor, Mozambique. *J. Land Use Sci.* **2018**, *13*, 325–343. [CrossRef]
8. Swette, B.; Lambin, E.F. Institutional changes drive land use transitions on rangelands: The case of grazing on public lands in the American West. *Glob. Environ. Chang.* **2021**, *66*, 102220. [CrossRef]
9. Kanianska, R.; Kizeková, M.; Nováček, J.; Zeman, M. Land-use and land-cover changes in rural areas during different political systems: A case study of Slovakia from 1782 to 2006. *Land Use Policy* **2014**, *36*, 554–566. [CrossRef]
10. Sun, P.; Xu, Y.; Wang, S. Terrain gradient effect analysis of land use change in poverty area around Beijing and Tianjin. *Trans. Chin. Soc. Agric. Eng.* **2014**, *30*, 277–288.
11. Saha, S.; Paul, G.; Hembram, T. Classification of terrain based on geo-environmental parameters and their relationship with land use/land cover in Bansloi River basin, Eastern India: RS/GIS approach. *Appl. Geom.* **2021**, *12*, 1–17. [CrossRef]
12. Zhang, L.; Hu, N. Spatial Variation and Terrain Gradient Effect of Ecosystem Services in Heihe River Basin over the Past 20 Years. *Sustainability* **2021**, *13*, 11271. [CrossRef]

13. Gitima, G.; Teshome, M.; Kassie, M.; Jakubus, M. Spatiotemporal land use and cover changes across agroecologies and slope gradients using geospatial technologies in Zoa watershed, Southwest Ethiopia. *Heliyon* **2022**, *8*, e10696. [CrossRef]
14. Martins, P.; Sano, E.; Martins, E.; Vieira, L.; Salemi, L.; Vasconcelos, V.; Júnior, A. Terrain units, land use and land cover, and gross primary productivity of the largest fluvial basin in the Brazilian Amazonia/Cerrado ecotone: The Araguaia River basin. *Appl. Geogr.* **2021**, *127*, 102379. [CrossRef]
15. Bai, S.; Chen, L.; Wang, L.; Shi, J.; Li, H. The impact of micro-topography on the land use pattern in the agro-pastoral ecotone. *Chin. Land Sci.* **2011**, *25*, 22–26. [CrossRef]
16. Chen, Z.; Huang, Y.; Zhu, Z.; Zheng, Q.; Que, C.; Dong, J. Landscape pattern evolution along terrain gradient in Fuzhou City, Fujian Province, China. *China. J. Appl. Ecol.* **2018**, *29*, 4135–4144. [CrossRef]
17. Liu, X.; Zhu, S.; Zhao, Y.; Li, R. Spatial-Temporal Evolution and Terrain Effects of Land Use Based on Geo-informatic Tupu in Hebei Shallow Mountainous Areas. *Geogr. Geo-Inf. Sci.* **2020**, *36*, 94–101.
18. Wang, X.; Dong, X.; Liu, H.; Wei, H.; Fan, W. Linking land use change, ecosystem services and human well-being: A case study of the Manas River Basin of Xinjiang, China. *Ecosyst. Serv.* **2017**, *27*, 113–123. [CrossRef]
19. Liu, C.; Xu, Y.; Lu, X. Spatiotemporal evolution and optimization of trade-off and synergy of land use functions in cologically fragile and poverty areas: A case study of Zhangjiakou City. *Econ. Geogr.* **2021**, *41*, 181–190. [CrossRef]
20. Liu, M.; Wang, Y.; Pei, H. The changes of land use and carbon storage in the northern farming-pastoral ecotone under the background of returning farmland to forest(grass). *J. Desert Res.* **2021**, *41*, 174–182.
21. Guo, H.; Xu, Y.; Wu, Y. Analysis of the land use spatial pattern and spatio-temporal changes based on terrain gradient: A case study of Pinggu District in Beijing. *Econ. Geogr.* **2013**, *33*, 160–167. [CrossRef]
22. Yang, A.; Zhu, L.; Chen, S.; Jin, H.; Xia, X. Geo-informatic spectrum analysis of land use change in the Manas River Basin, China during 1975–2015. *China J. Appl. Ecol.* **2019**, *30*, 3863–3874. [CrossRef]
23. Qu, Y.; Wang, S.; Zhu, W.; Ping, Z. Spatial-temporal differentiation characteristics and driving force of territorial space evolution in the Yellow River Delta. *Trans. Chin. Soc. Agric. Eng.* **2021**, *37*, 252–263+309.
24. Zhang, H.; Zhou, X.; Tang, G.; Zhou, L.; Ye, X. Hotspot discovery and its spatial pattern analysis for catering service in cities based on field model in GIS. *Geogr. Res.* **2020**, *39*, 354–369.
25. Xu, L.; Luo, W.; Zhou, B. Landscape Ecological Risk Assessment of Farming-Pastoral Ecozone Based on Land Use Change: A Case Study of the Yanghe Watershed, China. *J. Nat. Resour.* **2015**, *30*, 580–590.
26. Yin, X.; Sun, X.; Xu, X.; Zhang, X.; Chen, D. The impact of returning farmland on the soil conservation function in the Western Section of the Farming-pastoral Ecotone of Northern China. *J. Geo-Inf. Sci.* **2018**, *20*, 1721–1732.
27. Liu, B.; Yang, Y.; Li, Y. Quantitative analysis of land use structure characteristics over the farming-pastoral zone in the West Liaohe river basin, northern China. *J. Arid Land Resour. Environ.* **2018**, *32*, 64–71. [CrossRef]
28. Hu, J.; Hu, J.; Lv, Y. Spatial variation of the relationship between annual runoff and sediment yield and land uses based on the regional critical zone differentiation in the Loss Plateau. *Acta Eco. Sin.* **2021**, *41*, 1–13.
29. Li, S.; Shen, Z.; Liu, K.; Xu, Z.; Wang, H.; Jiao, S.; Liu, X.; Lei, Y. Analysis of terrain gradient effects of land use change in Daqing River Basin. *Trans. Chin. Soc. Agric. Eng.* **2021**, *37*, 275–284.
30. Guo, B.; Zhang, G. Land use change in farming-pastoral region of Inner Mongolia based on GIS and Markov model. *Trans. Chin. Soc. Agric. Eng.* **2009**, *25*, 291–298.
31. Yang, L.; Xie, Y.; Zong, L.; Qiu, T.; Jiao, J. Land Use Optimization Configuration based on Multi-Objective Genetic Algorithm and FLUS Model of Agro-pastoral Ecotone in Northwest China. *J. Geo-Inf. Sci.* **2020**, *22*, 568–579.
32. Wang, Y.; Gao, J.; Jin, Y.; Cao, B.; Wang, Y.; Zhang, X.; Zhou, J. Habitat Quality of Farming-pastoral Ecotone in Bairin Right Banner, Inner Mongolia Based on Land Use Change and InVEST Model From 2005 to 2015. *J. Ecol. Rural Environ.* **2020**, *36*, 654–662. [CrossRef]
33. Gao, J.; Luo, F.; Gao, Y.; Dang, X.; Meng, Z.; Chen, X.; Duan, N. Ecological soil C, N, and P stoichiometry of different land use patterns in the agriculture-pasture ecotone of Northern China. *Acta Ecol. Sin.* **2019**, *39*, 5594–5602.
34. Du, G.; Sun, X.; Liu, Y. Analysis of ecological restoration on ecosystem service and its human driving factors in Yan'an city. *Res. Soil Water Conserv.* **2016**, *23*, 233–239. [CrossRef]
35. Du, G.; Sun, X.; Liu, Y.; Zheng, H.; Ma, R. Temporal and spatial-differentiation characteristics of ecological restoration in Loess Plateau. *J. Geo-Inf. Sci.* **2017**, *19*, 355–364.
36. Sun, S.; Zhang, X. Analysis on the Spatiotemporal Evolution of Land Use Transformation and Its Ecological Environment Effect in Shaanxi Province. *Res. Soil Water Conserv.* **2021**, *28*, 1–9. [CrossRef]
37. Liu, C.; Huo, Y.; Xu, Y.; Huang, A.; Sun, P.; Lu, L. Changes in Cultivated Land and Influencing Factors before and after the Implementation of Grain for Green Project in Zhangjiakou City. *J. Nat. Resour.* **2018**, *33*, 1806–1820.
38. Sun, P.; Xu, Y.; Liu, Q.; Liu, C.; Huang, A. Spatiotemporal differentiation and driving factors of multi-functionality of land use in county scale in poverty belt around Beijing and Tianjin. *Trans. Chin. Soc. Agric. Eng* **2017**, *33*, 283–292.
39. Zhou, J.; Zhao, Y.; Huang, P.; Zhao, X.; Feng, W.; Li, Q.; Xue, D.; Dou, J.; Shi, W.; Wei, W.; et al. Impacts of ecological restoration projects on the ecosystem carbon storage of inland river basin in arid area, China. *Ecol. Indic.* **2020**, *118*, 106803. [CrossRef]
40. Wang, J.; Xu, X.; Liu, P. Land ues and land carrying capacity in ecotone between agriculture and animal husbandry in northern China. *Resour. Sci.* **1999**, *21*, 21–26.
41. Ma, L.; Li, T.; Li, T.; Long, D.; Chen, Y. Spatial distribution of rurality and types of rural development in farming-pastoral ecotone in Northern China. *Econ. Geogr.* **2015**, *35*, 126–133.

42. Fang, Z.; He, C.; Liu, Z.; Zhao, Y.; Yang, Y. Climate change and future trends in the Agro-Pastoral Transitional Zone in Northern China: The comprehensive analysis with the historical observation and the model simulation. *J. Nat. Resour.* **2020**, *35*, 358–370. [CrossRef]
43. Kong, D.; Chen, H. Spatio-temporal Patterns of Land Use Transitions and Related Influencing Factors-Comparative Analysis Based on Three Counties of North, Middle and South Jiangsu Province, China. *Chin. J. Soil Sci.* **2020**, *51*, 300–307. [CrossRef]
44. Peng, R.; Luo, Y.; Chen, Q.; Li, Y. Land use change and its driving mechanism in small-scale rocky desertification control area: Take the huajiang rocky desertification control area as an example. *Resour. Environ. Yangtze Basin* **2017**, *26*, 2073–2082.
45. Li, Y.; Yang, F.; Yang, L.; Shang, X.; Hu, G.; Jia, L. Spatial pattern changes and influencing factors of land use in Yulin City in the past 40 years. *Arid Land Geogr.* **2021**, *44*, 1011–1021.
46. Wang, J.; Xu, C. Geodetector: Principle and prospective. *Acta Geogr. Sin.* **2017**, *72*, 116–134.
47. Ma, S.; Qiao, Y.; Wang, L.; Zhang, J. Terrain gradient variations in ecosystem services of different vegetation types in mountainous regions: Vegetation resource conservation and sustainable development. *For. Ecol. Manag.* **2021**, *482*, 118856. [CrossRef]
48. Liu, D.; Li, L. Spatiotemporal change and driving factors of land use in the northern border transect of China, 1995-2015. *Resour. Sci.* **2021**, *43*, 1208–1221. [CrossRef]
49. Xu, Y.; Zhou, L.; Zhang, Z. Effect of cultivated land reclamation tracks on soil fertility changes in Changji Prefecture, Xinjiang. *Geogr. Res.* **2021**, *40*, 657–672.
50. Huang, A.; Xu, Y.; Sun, P.; Zhou, G.; Liu, C.; Lu, L.; Xiang, Y.; Wang, H. Land use/land cover changes and its impact on ecosystem services in ecologically fragile zone: A case study of Zhangjiakou City, Hebei Province, China. *Ecol. Indic.* **2019**, *104*, 604–614. [CrossRef]
51. Yu, Z.; Li, T.; Long, D.; Li, X.; Sun, D. The pattern evolution and it's reasons about the agricultural modernization in Shaanxi-Gansu-Ningxia region. *Sci. Geogr. Sin.* **2014**, *34*, 411–419.
52. Han, L.; Huo, H.; Liu, Z.; Zhao, Y.; Zhu, H.; Chen, R.; Zhao, Z. Spatial and temporal variations of vegetation coverage in the middle section of Yellow River Basin based on terrain gradient: Taking Yan'an City as an example. *China J. Appl. Ecol.* **2021**, *32*, 1581–1592. [CrossRef]
53. Song, Y.; Xue, D.; Xia, S.; Mi, W. Change characteristics and formation mechanism of the territorial spatial pattern in the Yellow River Basin from 1980 to 2018, China. *Geogr. Res.* **2021**, *40*, 1445–1463.
54. Shen, J.; Wang, X. Spatial-temporal changes in ecological risk of land use before and after Grain-for-Green policy in Zhengning County, Gansu Province. *J. Resour. Ecol.* **2013**, *4*, 36–42. [CrossRef]
55. Zhang, T.; Peng, J.; Liu, Y.; Zhao, M. Eco-geographical regionalization in Loess Plateau based on the dynamic consistency of vegetation. *Geogr. Res.* **2015**, *34*, 1643–1661.